High aboveground carbon stock of African tropical montane forests

Cuni-Sanchez, Aida

2021-08-25

other

acceptedVersion

High above-ground carbon stock of African tropical montane forests

Aida Cuni-Sanchez[1,2*], Martin J.P. Sullivan[3,4], Phil J. Platts[1,5], Simon L. Lewis[4,6], Rob Marchant[1], Gérard Imani[7], Wannes Hubau[8,9], Iveren Abiem[10,11], Hari Adhikari[12], Tomas Albrecht[13,14], Jan Altman[15], Christian Amani[7], Abreham B. Aneseyee[16,17], Valerio Avitabile[18], Lindsay Banin[19], Rodrigue Batumike[20], Marijn Bauters[21],Hans Beeckman[8], Serge K. Begne[4,22], Amy C. Bennett[4], Robert Bitariho[23], Pascal Boeckx[21], Jan Bogaert[24], Achim Bräuning[25], Franklin Bulonvu[26], Neil D. Burgess[27], Kim Calders[28], Colin Chapman[29-31], Hazel Chapman[11,33], James Comiskey[34], Thales de Haulleville[35], Mathieu Decuyper[36,37], Ben DeVries[38], Jiri Dolezal[15,39], Vincent Droissart[22,40], Corneille Ewango[41], Senbeta Feyera[42], Aster Gebrekirstos[43], Roy Gereau[44], Martin Gilpin[4], Dismas Hakizimana[45], Jefferson Hall[46], Alan Hamilton[47], Olivier Hardy[48], Terese Hart[49], Janne Heiskanen[12,50], Andreas Hemp[51], Martin Herold[37,52], Ulrike Hiltner[25,53], David Horak[54], Marie-Noel Kamdem[22], Charles Kayijamahe[55], David Kenfack[46], Mwangi J. Kinyanjui[56], Julia Klein[57], Janvier Lisingo[41], Jon Lovett[4], Mark Lung[58], Jean-Remy Makana[59], Yadvinder Malhi[60], Andrew Marshall[1,61,62], Emanuel H. Martin[63], Edward T.A. Mitchard[64], Alexandra Morel[65],John T. Mukendi[8], Tom Muller[66], Felix Nchu[67], Brigitte Nyirambangutse[68,69], Joseph Okello[21,70,71], Kelvin S.-H. Peh[72,73], Petri Pellikka[12,74], Oliver L. Phillips[4], Andrew Plumptre[75], Lan Qie[76], Francesco Rovero[77,78], Moses N. Sainge[79], Christine B. Schmitt[80,81], Ondrej Sedlacek[54], Alain S.K. Ngute[61,82], Douglas Sheil[83], Demisse Sheleme[84], Tibebu Y. Simegn[85], Murielle Simo-Droissart[22], Bonaventure Sonké[22], Teshome Soromessa[16], Terry Sunderland[86,87], Miroslav Svoboda[88], Hermann Taedoumg[89,90], James Taplin[91], David Taylor[92], Sean C. Thomas[93], Jonathan Timberlake[94], Darlington Tuagben[95], Peter Umunay[96], Eustrate Uzabaho[55], Hans Verbeeck[28], Jason Vleminckx[97],Göran Wallin[69], Charlotte Wheeler[64], Simon Willcock[98,99], John T. Woods[100], Etienne Zibera[68]

Abstract

Tropical forests store 40-50% of terrestrial vegetation carbon[1]. Spatial variations in aboveground live tree biomass carbon (AGC) stocks remain poorly understood, in particular in tropical montane forests[2]. Owing to climatic and soil changes with increasing elevation[3], AGC stocks are lower in tropical montane compared to lowland forests[2]. Here we assemble and analyse a dataset of structurally intact old-growth forests (AfriMont) spanning 44 montane sites in 12 African countries. We find that montane sites in the AfriMont plot network have a mean AGC-stock of 149.4 Mg C ha^{-1} (95% CI 137.1-164.2), comparable to lowland forests in the African Tropical Rainforest Observation Network[4] and about 70 per cent and 32 per cent higher than averages from plot networks in montane[2,5,6] and lowland[7] forests in the Neotropics, respectively. Notably, our results are two-thirds higher than the IPCC default values for these forests in Africa[8]. We find that the low stem density and high abundance of large trees of African lowland forests[4] is mirrored in the montane forests sampled. This carbon store is endangered: we estimate that 0.8 million ha of old-growth African montane forest have been lost since 2000. We provide country-specific montane forest AGC stock estimates modelled from our plot network to help guide forest conservation and reforestation interventions. Our findings highlight the need for conserving these biodiverse[9,10] and carbon-rich ecosystems.

43 **Main text**
44 Tropical forests cover less than 10% of the global land area yet store 40–50% of terrestrial
45 vegetation carbon[1] and contribute more than one third of primary productivity[11] so are a key
46 component of the global carbon cycle[12,13]. There is substantial variation in carbon stocks across the
47 biome, with lowland forests in Africa and Borneo storing more carbon per unit area than lowland
48 forests in the Neotropics[4,7]. This variation arises partly from structural differences: the signature
49 feature of African forests is their low stem density but relatively high abundance of large trees (>70
50 cm diameter) which store large quantities of carbon, while Bornean forests are characterised by high
51 stem density and basal area[4,14,15].
52
53 Despite increased understanding of biogeographic differences in tropical lowland forests, patterns of
54 spatial variation in carbon stocks remain poorly understood in the 880,000 km^2 of tropical montane
55 forests located ≥ 1,000 m asl[2]. Montane forests are expected *a priori* to have lower aboveground live
56 tree biomass carbon (AGC) stocks than lowland forests because (1) temperature decreases with
57 increasing elevation, reducing net primary productivity and slowing nutrient recycling, (2) long
58 periods of cloud immersion in montane forests suppresses productivity, (3) soil waterlogging slows
59 nutrient recycling and (4) high epiphyte load, local wind exposure in crests and nutrient-limited soils
60 limit tree size and increase investment in roots over shoots[3]. While forest inventory plots provide
61 some support for these assumptions[2] data from African mountain regions are exceptionally sparse.
62 Indeed, in the most recent IPCC guidelines, there is no specific AGC default value for old-growth
63 montane forests in Africa: the value given of 89.3 Mg C ha^{-1} is simply a mean of secondary and old-
64 growth forests found ≥ 1,000 m asl[8]. Mountain areas also pose special challenges for remote-sensing
65 approaches for estimating carbon stocks, as radar data are affected by geometric distortions[16] while
66 steep slopes bias spaceborne LiDAR estimates towards overestimating canopy height[17]. These issues
67 are reflected in the limited correlation between estimates of AGC-stocks at mountain locations from
68 different recent remote-sensing derived carbon maps (Supplementary Information Table S1).
69
70 Better understanding of montane carbon stocks is important for many African countries, particularly
71 in eastern Africa where montane forests represent most of the extant evergreen old-growth forest
72 cover. Quantifying carbon stocks in these ecosystems is critical for estimating national carbon losses
73 from deforestation and forest degradation[18]. Quantifying carbon stocks in old-growth montane
74 forests also serves to constrain potential carbon uptake by restored natural forests, given the high
75 commitment of most African nations to the Bonn Challenge effort to restore 150 million ha of
76 degraded and deforested lands by 2020 (see Table 1), and 350 million by 2030.
77
78 Here we measured, compiled and analysed a new dataset of 226 plot inventories spanning 44 sites
79 in 12 African countries, covering most major mountain regions on the continent (the "AfriMont"
80 dataset). Plots range from 800 to 3,900 m asl to include submontane forests (800-1,000 m asl) in
81 smaller mountains closer to the ocean[19,20]. For all plots, stem diameter and species were recorded
82 for each tree ≥10 cm diameter at breast height (or above buttress) following standard methods[21].
83 Tree height was sampled in 23 montane sites, allowing variation in height-diameter allometry to be
84 incorporated into the calculation of aboveground biomass. A total of 72,336 stems with diameter
85 ≥10 cm were measured. For each tree, we computed AGC (in Mg C ha^{-1}) according to standard
86 procedures (see methods).
87
88 We find that the mean plot-level AGC-stock across sampled African tropical montane forests is 149.4
89 Mg C ha^{-1} (95% confidence interval (CI) 137.1-164.2), two-thirds more than the IPCC default value of
90 89.3 Mg C ha^{-1}. Our estimates are robust to subsampling our dataset (Extended Data Fig. 1) and
91 excluding small plots (Extended Data Fig. 2) and are not affected by the sampling strategy used to
92 establish plots in each study site (Extended Data Fig. 2). Comparing our dataset to previous
93 syntheses of montane[2,5,6] and lowland[7] forest plot networks reveals that tropical montane forests in

94   Africa have significantly higher AGC-stocks per unit area than both montane (95% CI = 50.4 – 71.9
95   Mg C ha^{-1}) and lowland (95% CI = 124.0 – 147.9 Mg C ha^{-1}) forests in the Neotropics, and that they
96   do not differ significantly from lowland forests in Africa (95% CI = -27.6 – 9.6 Mg C ha^{-1}) (Fig. 1, Table
97   S2). The similar AGC-stocks in montane and lowland forests in Africa contrasts with the Neotropics
98   and Southeast Asia, where carbon stocks are lower in montane forests than lowland forests (albeit
99   not significantly different in Southeast Asia due to the small sample size, Fig. 1). These differences
100   are robust to accounting for differences in elevation among montane datasets: removing African
101   plots 800-1,000 m asl slightly reduces estimated montane forest AGC-stock to 145.0 Mg C ha^{-1} (95%
102   CI 129.6 – 163.2), but observed differences in AGC-stock among continents remain when plots are
103   restricted to elevations well represented in all continents (Extended Data Fig. 3).

105   The characteristic structural properties of lowland African forests (relatively low stem density and
106   greater importance of large trees compared to elsewhere in the tropics[4]) are also evident in the
107   African montane forests we sampled. In these montane forests mean stem density is 483.3 stems ha^{-1}
108   (± 177.7 s.d.) and mean basal area is 39 m^{2}ha^{-1} (± 14.8 s.d.). We find a high density of large stems
109   (>70 cm diameter, 19.1 stems ha^{-1}± 15.4 s.d.) which contribute 35.3% (95% CI = 29.6 – 41.8 %) to
110   plot-level AGC-stock (Fig. 2). The contribution of large trees to plot-level AGC-stock is also similar in
111   montane and lowland Africa (95% CI of difference in square-root transformed proportional
112   contribution of large trees between lowland and montane forests = -0.100 - 0.075, P = 0.80). There
113   was no significant difference in the proportional contribution of any other size class to AGC-stocks
114   between our montane dataset and 132 lowland plots from the AfriTRON network (P≥0.24, Table S3),
115   although greater variation among plots is observed in montane forests (Fig. 2).

117   To investigate if elevation affected AGC or forest structure, we modelled these variables as functions
118   of elevation using random slopes mixed-effects models. This approach allows intercepts and
119   relationships to vary among sites, which would be expected as mountains can have very different
120   climate at the same elevation due to proximity to the ocean (generally the further, the drier) and
121   because of the mass-elevation or telescopic effect[22] (larger mountains are better at warming the
122   atmosphere above them). We found that AGC, stem density or density of large stems (>70 cm
123   diameter) were not significantly related to elevation (Fig. 3, Table S4). Across sites these non-
124   significant relationships were all negative, although there was some variation in strength and
125   direction amongst sites (Fig. 3). Similarly, in the Neotropics and Southeast Asia montane forest plot
126   datasets, AGC was not significantly correlated with elevation (Extended Data Fig. 4).

128   To assess potential environmental drivers of AGC-stock variation across the AfriMont plot network,
129   we related AGC to climate, soil and topography. We found that AGC-stocks increased with annual
130   precipitation (albeit not statistically significantly), decreased with soil fertility and were higher in
131   plots which were locally at higher elevation than their surroundings (Extended Data Fig. 5).
132   Relationships with other environmental variables were non-significant (Extended Data Fig. 5).
133   Although global datasets might not capture fine-scale variation in climate or soils in mountain
134   regions[23], leading to regression dilution[24], the general absence of strong climate effects combined
135   with the lack of significant effect of elevation on AGC-stocks suggest that the high AGC-stock of
136   African montane forests is a pervasive phenomenon across a wide environmental gradient.

138   Although the AfriMont dataset covers most major mountain areas in tropical Africa (Fig. 4), some
139   areas remain under-sampled relative to forest extents (Extended Data Fig. 6), resulting in some
140   differences between the environmental conditions sampled by our plot network and the wider
141   montane forest biome in Africa (Extended Data Fig. 7). Notably, the absence of plots from montane
142   forests of eastern Democratic Republic of the Congo (Fig. 4, Extended Data Fig. 6) means that the
143   AfriMont dataset samples forests are, on average, at higher elevations, and that are cooler and
144   cloudier than the wider montane forest biome in Africa (Extended Data Fig. 7). Using relationships

145 with environmental variables (Extended Data Fig. 5) to predict AGC-stocks in each 1-km grid cell
146 containing montane forest gives a mean (weighted by remaining forest cover) AGC-stock of 176.9
147 Mg C ha^{-1} (± 32.0 s.d.) for the tropical montane forest biome in Africa. This indicates that the
148 estimate we report based on our AfriMont plot network data (149.4 Mg C ha^{-1}) is conservative.

150 Several mechanisms could explain the high AGC-stock of montane forests in the AfriMont plot
151 network. Firstly, large herbivores such as elephants (*Loxodonta* spp.) can have profound effects on
152 forest structure by consuming biomass, destroying small stems, dispersing seeds and transporting
153 nutrients[25]. Studies for lowland forests suggest that elephants can increase carbon stocks[26,27]. We
154 tested if AfriMont plots with known elephant presence as of 2019 had significantly higher AGC-
155 stocks, but found that they had significantly lower AGC-stocks, although significant differences were
156 not observed in some countries (Extended Data Fig. 8). While the initial ecosystem response to
157 elephant removal might be greater AGC-stocks due to reduced biomass consumption and small-stem
158 destruction, the longer-term effects might differ. We were unable to fully disentangle such effects,
159 as we lacked details on both i) time since elephant extirpation, and ii) elephant abundance and its
160 determinants (see Table S5).

162 A second potential explanation is a relatively low frequency of large-scale abiotic disturbances,
163 allowing trees time to grow large and stands to self-thin, as is seen in lowland African forests[4]. For
164 example, tropical cyclones are largely absent in mainland Africa (except in Mozambique[28]) and lava
165 flows are limited even in the active volcano of Mt Cameroon[29]. Although fine-scale variability in
166 landslide risk limits comparisons across large spatial scales, there are fewer areas with high landslide
167 susceptibility in mountains in tropical Africa than in the Andes and most mountain ranges in
168 Southeast Asia[30]. If forests have been ecologically stable over evolutionary timescales, tree species
169 may be adapted to grow slowly but potentially reaching great sizes[31]. On Mt Kilimanjaro
170 *Entandrophragma* individuals reach enormous heights and ages[32]. This low frequency of large-scale
171 abiotic disturbances contrasts with the Andes and several mountains in Southeast Asia (e.g. Barisian
172 mountains in western Sumatra), which are tectonically active, so the trees there are adapted to
173 sudden disturbance followed by intense competition to get established and grow. Future monitoring
174 of the AfriMont plot network will help determine the extent to which the high biomass of African
175 tropical montane forests results from them being dynamic and productive, or adapted to stability.

177 A third potential explanation could be the presence of conifers[33]. Mixed conifer/broad-leaved forests
178 tend to have greater basal area than purely broad-leaved forests due to a more effective use of light
179 and other resources[34]. Podocarpaceae can be found in montane forests across the tropics[35]. Despite
180 having fewer species in Africa than in other continents[36], these could be more abundant at the site-
181 level. However, there is no pantropical comparative study on Podocarpaceae abundance in tropical
182 montane forests. In our dataset there was no significant correlation between plot-level AGC-stock
183 and conifer (Podocarpaceae) abundance (Extended Data Fig. 9). Other explanations could be
184 continental differences in mountain terrain (more gentle slopes or plateau regions in Africa) or types
185 of montane forests investigated (less cloud forest existing/sampled in Africa). Within our dataset,
186 slope did not have a significant effect on AGC-stocks (Extended Data Fig. 5). Contrary to the
187 Neotropics[37], there is no high-resolution map of cloud forests available for Africa, so while we found
188 no relationship between AGC-stock and cloud frequency (Extended Data Fig. 5), we were unable to
189 investigate differences in AGC-stock between cloud forest vs non-cloud forest plots.

191 To understand the policy implications of our findings for African countries, we calculated montane
192 (≥800 m asl) forest cover change between 2000 and 2018, using forest cover from ref.[38] clipped to
193 'primary humid forest' from ref.[39]. We show that tropical montane forests represent most -or all-
194 evergreen old-growth forests found in ten African countries (Fig. 4), and that the Democratic
195 Republic of the Congo has two thirds of the remaining 16 million ha of montane forests in Africa.

196   Over 0.8 million ha (5%) have been lost in Africa since 2001, with the highest losses in the
197   Democratic Republic of the Congo (536,000 ha), Uganda (65,000 ha) and Ethiopia (62,000 ha) (Fig. 4,
198   Table 1). In terms of percentage, Mozambique and Côte d'Ivoire lost over 20% of their montane
199   forests over this period (Fig. 4, Table 1). In some sites, however, a larger proportion of montane
200   forests was lost before 2000, e.g. in Taita Hills in Kenya[40]. If absolute country-level deforestation
201   rates continue, a further 0.5 million ha of tropical montane forests will be lost by 2030.

203   African tropical montane forests are not only carbon-rich, but they also harbour some of the highest
204   concentrations of biodiversity and endemism in the world[9,10]. They are important 'water towers' as,
205   located at the headwaters of numerous river systems, including the Congo and the Nile, they
206   regulate timing and magnitude of runoff[9]. They also regulate local temperatures[41] and provide
207   numerous other services to people in the surrounding landscapes[9]. Clearly, more should be done to
208   avoid the destruction of these important ecosystems. Logging, mining and clearing land for farming,
209   but also political unrest and militia presence have affected -and continue to affect- these forests, e.g.
210   in Itombwe Mts in the Democratic Republic of the Congo[42]. Protected areas are known to help
211   reduce deforestation in the tropics[43]. Beyond protected areas, other forest conservation
212   mechanisms could be implemented, including effective carbon finance. Previous IPCC AGC-stock
213   estimates for montane forests in Africa (89.3 Mg C ha^{-1}) may have contributed to low incentives for
214   carbon finance mechanisms in these ecosystems. Our study shows the far greater carbon storage
215   potential in these tropical montane forests, which will be even higher if soil carbon stocks are
216   considered (e.g. > 200 Mg C ha^{-1} of organic carbon occurs in the top 0-30 cm soil on Mt Cameroon[44]
217   and in the Usambara Mts, Tanzania[45]).

219   As well as conserving the remaining montane forests, efforts to restore them are critical. Forest
220   restoration at one of our sites, Kibale National Park in Uganda, indicates the potential for rapid AGC
221   accumulation[46]. Our study shows the high potential AGC-stock these montane forests can attain. The
222   possible co-benefits of forest restoration, notably water regulation, control of soil erosion and
223   landslides and biodiversity conservation should also be considered. Most African nations are
224   committed to the Bonn Challenge; Ethiopia leading with 15 million ha committed (Table 1). We
225   provide country-specific estimates of potential AGC-stocks based on forests sampled in the AfriMont
226   dataset to help guide such interventions (Table 1, Extended Data Fig. 10). Caution is needed when
227   scaling-up our estimates to the landscape scale, as not all forests are closed-canopy old-growth and
228   structurally intact. Remote sensing or ancillary data (landcover maps, spatial environmental data)
229   could be used to identify e.g. exotic plantations, degraded or bamboo forests, and thus help create
230   detailed AGC maps at different spatial scales[18,47]. A closer collaboration between air-borne, space-
231   borne and ground approaches (such as the AfriMont and AfriTRON plot networks) is key for accurate
232   quantification and monitoring of landscape-scale tropical forest AGC-stocks, particularly in mountain
233   regions.

235   Our newly compiled dataset and analysis provides a large-scale quantification of AGC-stock in
236   African tropical montane forests, indicating it to be on average substantially higher than previously
237   thought. While there is variation around this mean AGC-stock within and across sites, it is not
238   systematically related to elevation. Apart from helping refine country-level estimates, IPCC
239   guidelines and ground-calibration of remote-sensing estimates, continued on-the-ground monitoring
240   of the AfriMont plot network will help determine ecosystem dynamics and carbon residence time in
241   these extraordinarily carbon-rich forests, as well as their responses to climatic changes.

Figures main document
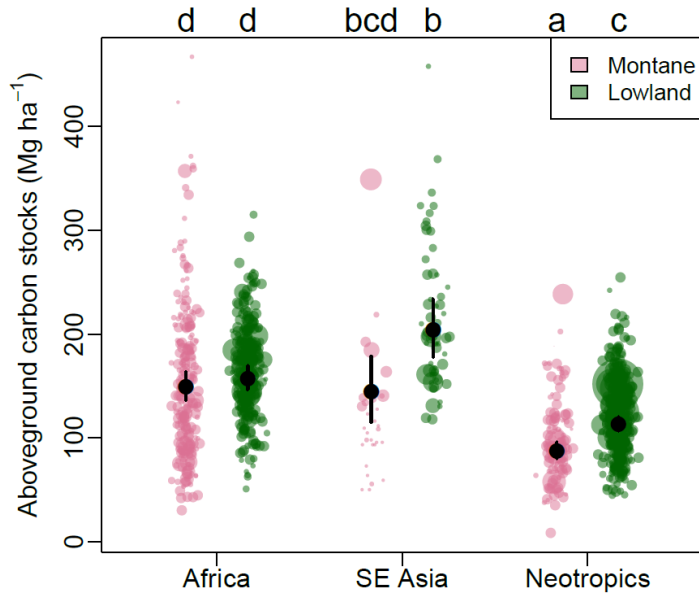
Fig. 1 | Pantropical variation in aboveground carbon stocks sampled by plot networks in montane (≥ 800 m asl) and lowland (< 800 m asl) tropical forests. Data from this study for African montane forests (*n* = 226 plots, this study), montane forests in the Neotropics (*n* = 131) and Southeast Asia (*n* = 32) are from ref.[2,5,6], lowland forests in Africa (*n* = 290), the Neotropics (*n* = 416) and Southeast Asia (*n* = 60) arewfrom ref.[7]. Coloured points show the AGC-stock in each plot, with point size proportional to square-root plot area. Black points show means for each continent-elevation category estimated using linear mixed-effects models with site as a random effect, and lines show 95% confidence intervals around means. Letters indicate signficiant differences between continent elevation category combinations (linear mixed-effects models with site as a random effect, *P* < 0.05).
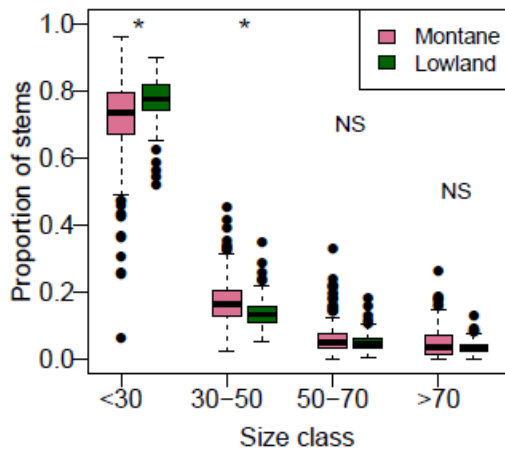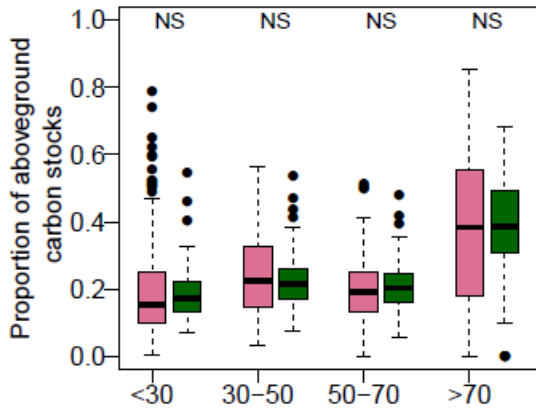
258
259 **Fig. 2 | Proportion of plot-level aboveground carbon stock and stems accounted for by each size**
260 **class in montane and in lowland forests in Africa.** Statistically significant differences in contribution
261 of each size class between montane and lowland forest plot networks are shown by asterisks (linear
262 mixed-effects model, $P < 0.05$). NS = non-significant difference. Montane ($n = 226$), lowland ($n =$
263 132). The thick line shows the median, and boxes cover the interquartile range (IQR). Values > 1.5
264 times IQR away from the IQR are shown by points.
265
266
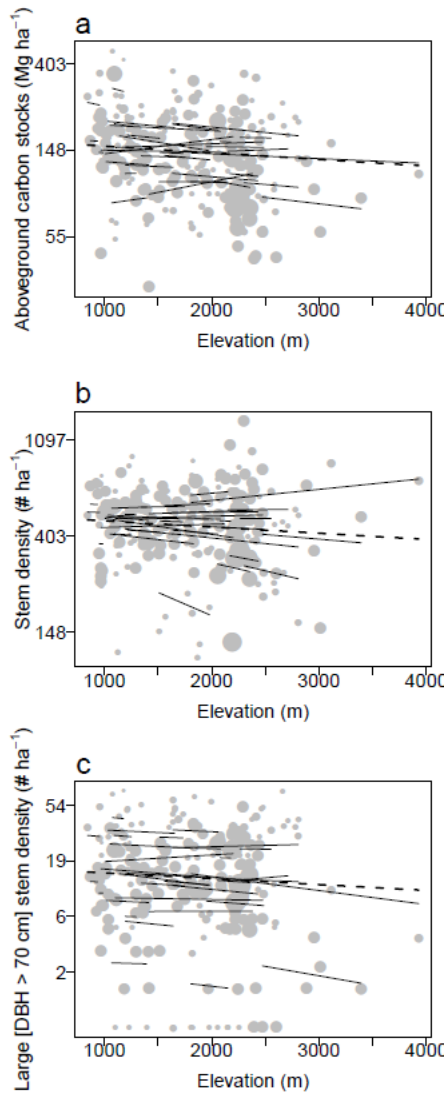
267
268 **Fig. 3 | Variables as a function of elevation.** a-c Relationship between elevation and plot-level AGC
269 stock (a), stem density (b) and stem density of large stems (>70 cm diameter; c) for the AfriMont
270 dataset. Note log-scale of y-axis. Each response variable was log-transformed and modelled as a
271 function of elevation with a linear mixed-effect models with random slopes. The dashed line shows
272 the relationship across sites (non-significant in all cases, $P \geq 0.3$, Table S4), while the black lines show
273 the relationship within each site. Point sizes are proportional to square-root plot area. A polynomial
274 model allowing a non-linear relationship with elevation was also tested but not supported over the
275 linear model in any case ($P \geq 0.7$, Table S4). The absence of a significant relationship with elevation is
276 robust to removing the two highest elevation sites, Rwenzori and Virunga (Table S4). DBH diameter
277 at breast height.

278
279
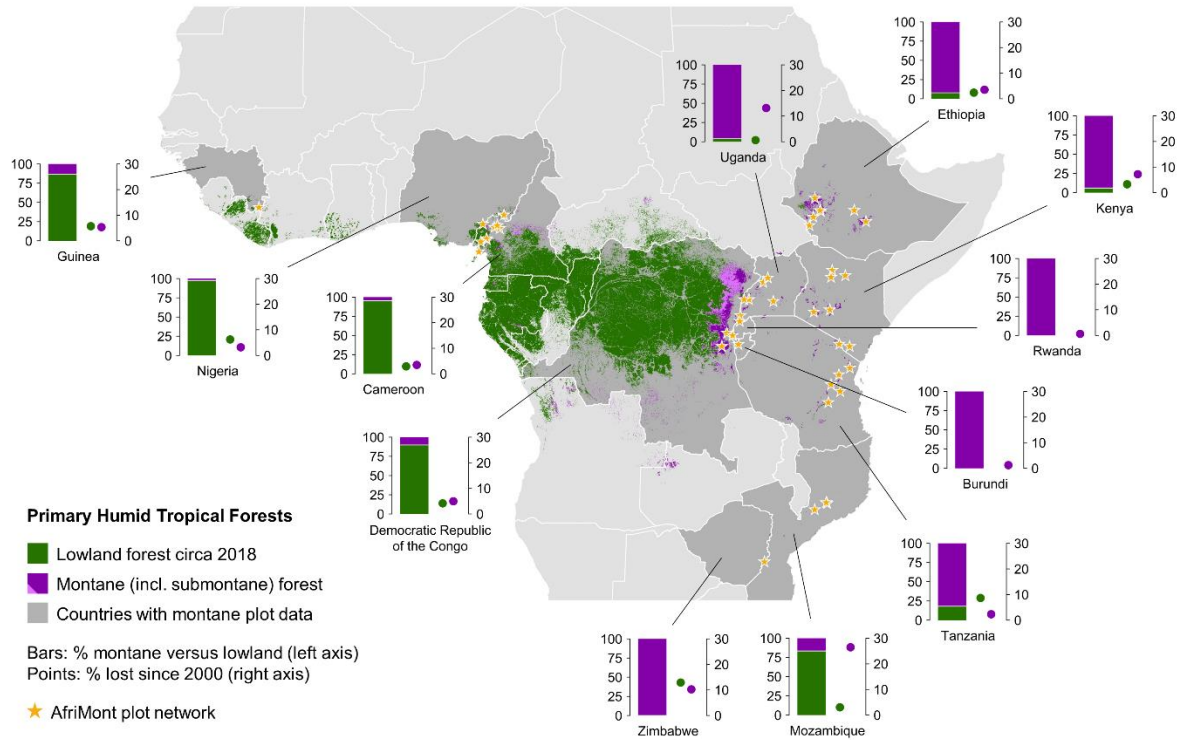
280
281 **Fig. 4. | Old-growth evergreen humid forests in lowland and montane tropical Africa.** Forest
282 extends circa 2018. Note that montane includes submontane forests (800-1,000 m asl, light purple).
283 Montane forests represent most (or all) evergreen humid old-growth forest in ten African nations:
284 Burundi, Ethiopia, Kenya, Rwanda, Tanzania, Uganda and Zimbabwe (included in AfriMont); and
285 Zambia, Malawi and South Sudan (no plot data available). Forest cover extracted from ref.[38] and
286 clipped to 'primary humid forest' using ref.[39]. See Table 1 for country-level absolute estimates.
287

288 **Table 1 | Remaining forest area and aboveground carbon estimates for montane and lowland**
289 **tropical forests in Africa**

290

Country	Montane (ha)	Montane lost (ha)	Montane AGC (MgC ha⁻¹, 95% CI)	Montane sites (plots)	Lowland (ha)	Lowland AGC (MgC ha⁻¹, 95% CI)	Lowland plots	Bonn Challenge by 2020 (ha)
Burundi	25,000	300	**94** (47-176)	1 (7)	0		0	2 million
Cameroon	840,000	30,200	**153** (121-195)	7 (37)	17.7 million	**166** (151-185)	72	12 million
DRC	10.2 million	536,500	**129** (84-202)	2 (37)	90 million	**158** (135-183)	48	8 million
Ethiopia	1.7 million	62,100	**165** (124-215)	8 (25)	145,000	ᵃ	0	15 million
Guinea	29,000	1,700	**314** (147-616)[b]	1 (2)	193,000	**157** (122 – 206)[c]	24	2 million
Kenya	568,000	44,100	**104** (79-136)	8 (38)	37,000		0	5.1 million
Mozambique	18,000	6,600 [d]	**226** (146-384) [b]	3 (4)	93,000	ᵉ	0	1 million
Nigeria	42,000	1,400	**120** (47-309) [b]	1 (1)	1.8 million	**161** (105-262)	2	4 million
Rwanda	53,000	300	**106** (65-168)	2 (11)	0		0	2 million
Tanzania	587,000	13,900	**175** (129-234)	6 (29)	130,000	**128** (101-163)	16	5.2 million
Uganda	427,000	64,600 [d]	**158** (111-209)	6 (23)	18,000		0	2.5 million
Zimbabwe	7,000	800 [d]	**203** (108-363)	1 (12)	<1,000		0	2 million

291

292 Forest cover circa 2018 was extracted from ref.[38] and clipped to 'primary humid forest' using ref.[39].
293 Montane forest lost covers the period 2000-2018. Mean aboveground carbon (AGC, in MgC ha⁻¹)
294 estimates for montane (or lowland) forests were estimated from AfriMont and AfriTRON plot
295 network data. Mean AGC values are in boldface, 95% confidence intervals in parentheses. For details
296 on sites and plots used see Table S5. Bonn Challenge pledges for 2030 not yet available.
297 ᵃ Ref.[48] report 192 MgC ha⁻¹ for lowland.
298 ᵇ Few plots sampled, or very small plots sampled, AGC estimates may not be robust, see Extended
299 data Fig. 10.
300 ᶜ Data from neighbouring Liberia.
301 ᵈMontane forest loss in Mozambique, Uganda and Zimbabwe represents 27%, 13% and 10% of the
302 existing montane forest in 2001, respectively. Montane forest loss in Côte d'Ivoire (no plot data
303 available) was estimated to be 21% for the same period.
304 ᵉ Ref.[49] report 132.2 MgC ha⁻¹ for lowland.

305

306

References

1. Erb, K., et al. Unexpectedly large impact of forest management and grazing on global vegetation biomass. *Nature* **553**, 73–76 (2018).
2. Spracklen, D.V. & Righelato, R. Tropical montane forests are a larger than expected global carbon store. *Biogeosciences* **11**, 2741-2754 (2014).
3. Fahey, T. J., Sherman, R. E. & Tanne, E. V. J. Tropical montane cloud forest: environmental drivers of vegetation structure and ecosystem function. *J. Trop. Ecol.* **32**, 355–367 (2016).
4. Lewis, S. L. et al. Above-ground biomass and structure of 260 African tropical forests. *Phil. Trans. R. Soc. Lond. B* **368**, 20120295 (2013).
5. Vilanova, E. et al. Environmental drivers of forest structure and stem turnover across Venezuelan tropical forests. *PLoS ONE* **13**(6): e0198489 (2018).
6. Alvarez-Davila, E. et al. Forest biomass density across large climate gradients in northern South America is related to water availability but not with temperature. *PLoS ONE* **12**(3): e0171072 (2017).
7. Sullivan, M. J. P., et al. Long-term thermal sensitivity of Earth's tropical forests. *Science* **368**, 869–874 (2020).
8. Domke, G. et al. in 2019 Refinement to the 2006 IPCC Guidelines for National Greenhouse Gas Inventories Vol. 4 (eds Calvo Buendia, E. et al.) Ch. 4, 48 (IPCC, 2019).
9. *African Mountains Atlas* (UNEP, 2014).
10. Rahbek, C., et al. Humboldt's enigma: What causes global patterns of mountain biodiversity? *Science* **365**, 1108–1113 (2019).
11. Pan, Y. et al. A large and persistent carbon sink in the world's forests. *Science* **333**, 988–993 (2011).
12. Booth, B. B. B. et al. High sensitivity of future global warming to land carbon cycle processes. *Environ. Res. Lett.* **7**, 024002 (2012).
13. Hubau, W., et al. Asynchronous carbon sink saturation in African and Amazonian tropical forests. *Nature* **579**, 80–87 (2020).
14. Feldpausch, T. R. et al. Tree height integrated into pantropical forest biomass estimates. *Biogeosciences* **9**, 3381–3403 (2012).
15. Bastin, J.-F., et al. Pan-tropical prediction of forest structure from the largest trees. *Global Ecol. Biogeogr.* **27**, 1366–1383 (2018).
16. CCI BIOMASS Product User Guide Year 1 Version 1.0. (Aberystwyth University and GAMMA Remote Sensing, 2019) https://climate.esa.int/sites/default/files/biomass_D4.3_Product_User_Guide_V1.0.pdf
17. Lefsky, M. A., Keller, M., Pang, Y., de Camargo, P. & Hunter, M. O. Revised method for forest canopy height estimation from the Geoscience Laser Altimeter System waveforms. J. *Appl. Remote Sens.* **1**, 013537 (2007).
18. Willcock, S., et al. Quantifying and understanding carbon storage and sequestration within the Eastern Arc Mountains of Tanzania, a tropical biodiversity hotspot. *Carbon Balance Manage.* **9**, 2 (2014).
19. Bussmann, R.W. Vegetation zonation and nomenclature of African Mountains – An overview. *Lyonia* **11**, 41–66 (2006).
20. Hamilton, A. Vegetation, climate and soil, altitudinal relationships on the East Usambara Mountains of Tanzania. *J. E. Afr. Nat. Hist.* **87**, 1-5 (1998).
21. Phillips, O., Baker, T., Brienen, R. & Feldpausch, T. RAINFOR field manual for plot establishment and remeasurement. http://www.rainfor.org/upload/ManualsEnglish/RAINFOR_field_manual_version_2016.pdf (Univ. Leeds, 2016).
22. Jarvis, A. & Mulligan, M., The climate of cloud forests. *Hydrol. Process.* **25**, 327–343 (2011).
23. Platts, P.J., Omeny, P.A. & Marchant, R. AFRICLIM: high-resolution climate projections for ecological applications in Africa. *Afr. J. Ecol.* **53**, 103–108 (2015).

358   24. McInerny, G. J., Purves, D. W. Fine-scale environmental variation in species distribution
359   modelling: Regression dilution, latent variables and neighbourly advice. *Methods Ecol. Evol.*
360   **2**, 248–257 (2011).
361   25. Poulsen, J.R., et al. Ecological consequences of forest elephant declines for Afrotropical
362   forests. *Conserv. Biol.* **32**, 559–567 (2018).
363   26. Berzaghi, F., et al. Carbon stocks in central African forests enhanced by elephant
364   disturbance. *Nat. Geosci.* **12**, 725–729 (2019).
365   27. Enquist, B.J., et al. The megabiota are disproportionately important for biosphere
366   functioning. *Nat. Commun.* **11**, 699 (2020).
367   28. Lin, T.-C., Hogan, J.A. & Chang, C.T. Tropical Cyclone Ecology: A Scale-Link Perspective.
368   *Trends Ecol. Evol.* **35**, 594–604 (2020).
369   29. Favalli, M., et al. Lava flow hazard and risk at Mt. Cameroon volcano. *Bull. Volcanol.* **74**, 423–
370   439 (2012).
371   30. Stanley, T. & Kirschbaum, D.B. A heuristic approach to global landslide susceptibility
372   mapping. *Nat. Hazards* **87**, 145–164 (2017).
373   31. Lovett, J. C. Elevational and latitudinal changes in tree associations and diversity in the
374   Eastern Arc mountains of Tanzania. *J. Trop. Ecol.* **12**, 629–650 (1996).
375   32. Hemp, A., et al. Africa's highest mountain harbours Africa's tallest trees. *Biodiv. Conserv.* 26,
376   103–113 (2016).
377   33. Culmsee, H., Leuschner, C., Moser, G. & Pitopang, R., Forest aboveground biomass along an
378   elevational transect in Sulawesi, Indonesia, and the role of Fagaceae in tropical montane rain
379   forests. *J. Biogeogr.* **37**, 960–974 (2010).
380   34. Enright, N.J. & Ogden, J. The southern conifers - a synthesis. Ecology of the southern conifers
381   (ed. by N.J. Enright & Hill R.S.), pp. 271–287. Melbourne University Press, Melbourne (1995).
382   35. Neale, D. B. & Wheeler, N. C. The Conifers. In: The Conifers: Genomes, Variation and
383   Evolution (eds. Neale, D. B. & Wheeler, N. C.) pp 1–21. Springer International Publishing
384   (2019).
385   36. Mill, R. R. Towards a Biogeography of the Podocarpaceae. In IV International Conifer
386   Conference, R. R. Mill, ed. *Acta Hort.* **615**, 137–147 (2003).
387   37. Helmer, E.H., Gerson, E.A., Baggett, L.S., Bird, B.J., Ruzycki, T.S. & Voggesser, S.M.
388   Neotropical cloud forests and paramo to contract and dry from declines in cloud immersion
389   and frost. PLoS ONE **14**(4): e0213155 (2019).
390   38. Hansen, M. C., et al. High-Resolution Global Maps of 21st-Century Forest Cover Change.
391   *Science* **342**, 850-853 (2013).
392   39. Turubanova, S., Potapov, P., Tyukavina, A. & Hansen M. Ongoing primary forest loss in Brazil,
393   Democratic Republic of the Congo, and Indonesia. *Environ. Res. Lett.* **13**, 074028 (2018).
394   40. Pellikka, P. K. E., Lötjönen, M., Siljander, M. & Lens, L. Airborne remote sensing of
395   spatiotemporal change (1955–2004) in indigenous and exotic forest cover in the Taita Hills,
396   Kenya. *Int. J. Appl. Earth Obs.* **11**, 221–232 (2009).
397   41. Zeng, Z. et al. Deforestation-induced warming over tropical mountain regions regulated by
398   elevation. *Nat. Geosci.* **14**, 23–29 (2020). https://doi.org/10.1038/s41561-020-00666-0
399   42. Spira, C., Kirkby, A., Kujirakwinja, D. & Plumptre, A. J. The socio-economics of artisanal
400   mining and bushmeat hunting around protected areas: Kahuzi– Biega National Park and
401   Itombwe nature reserve, eastern Democratic Republic of Congo. *Oryx* **53**, 136–144(2017).
402   43. Bebber, D.P. & Butt, N. Tropical protected areas reduced deforestation carbon emissions by
403   one third from 2000-2012. *Sci. Rep.* **7**, 14005 (2017).
404   44. Tegha, K. C. & Sendze, Y. G., Soil organic carbon stocks in Mt Cameroon National Park under
405   different land uses. *J. Ecol. Nat. Environ.* **8**, 20–30, (2016).
406   45. Munishi, P.K.T. & Shear, T.H. Carbon storage in afromontane rain forests of the eastern arc
407   mountains of Tanzania: their net contribution to atmospheric carbon. *J. Trop. For. Sci.* **16**,
408   78–98 (2004).

409   46. Wheeler, C.E., et al. Carbon sequestration and biodiversity following 18 years of active
410   tropical forest restoration. *Forest Ecol. Manage.* **373**, 44–55 (2016).
411   47. Avitabile, V., Baccini, A., Friedl, M.A. & Schmullius, C. Capabilities and limitations of Landsat
412   and land cover data for aboveground woody biomass estimation of Uganda. *Remote Sens.*
413   *Environ.* **117**, 366–380 (2012).
414   48. Aneseyee, B A., Soromessa, T. & Belliethathan, S. Carbon Sock of Gambella National Park:
415   Implication for Climate Change Mitigation. *Int. J. Adv. Life Sci.* **35**, 41–56 (2015).
416   49. Lisboa, S.N., et al. Biomass allometric equation and expansion factor for a mountain moist
417   evergreen forest in Mozambique. *Carbon Balance Manage.* **13**, 23 (2018).

418

419   **Methods**
420   **AfriMont or montane Africa dataset**
421   We compiled forest inventory plot data from the African Tropical Rainforest Observatory Network
422   (AfriTRON; www.afritron.org), with data curated at www.ForestPlots.net[50,51] and the TEAM
423   network[52], as well as from numerous site-specific publications detailed in Table S5 and mapped in
424   Fig. 4. Plots were selected for the analysis when conforming to the following criteria: ≥800 m asl,
425   closed-canopy evergreen wet or moist tropical forest, geo-referenced, old-growth and structurally
426   intact (not impacted by recent selective logging, fire or coffee cultivation), with no exotic species
427   present (e.g. *Eucalyptus* or *Pinus* spp.), all trees ≥10 cm diameter measured and majority of stems
428   identified to species. We included plots from Virunga Massif in Rwanda/Uganda even when not
429   100% closed-canopy due to high abundance of naturally-occurring bamboo. In all plots, tree
430   diameter was measured at 1.3 m along the stem from the ground, or above buttresses if present. In
431   23 sites tree height was sampled in the field for some stems, using a clinometer or a laser. Families
432   and species names follow the African Plant Database (http://africanplantdatabase.ch). The AfriMont
433   dataset consists of 72,336 stems, of which 92.9% were identified to species, 98.4% to genus and
434   98.5% to family. This dataset represents a standardised safe long-term repository of valuable
435   historical data (four sites initially considered could not be included because tree-level data had
436   already been lost by data owners).

437

438   **AfriTRON or lowland Africa dataset**
439   The 132 lowland-forest plots are all from AfriTRON[4,13,53]. They were selected using the same criteria
440   as above (but with elevation <800 m asl), restricted to countries for which we also had montane
441   plots plus neighbouring countries where the mountains span international borders (e.g. Mt Nimba
442   spans Guinea and Liberia). The dataset includes 51,305 stems, of which 89.6% were identified to
443   species, 97.3% to genus and 97.7 % to family. The plot data were retrieved from forestplot.net on
444   06/01/2019. The plot locations and details are in Table S6.

445

446   **Literature dataset**
447   We compiled data on AGC-stocks in tropical lowland and montane forests to compare to the
448   AfriMont data. Data for lowland forests came from ref.[7] and consisted of all multi- and single-census
449   plots that were <800 m asl. Data for montane forests were obtained from ref.[2], with additional data
450   from Venezuela (ref.[5]) and Colombia (ref.[6]). Montane plots were defined as ≥800 m asl; elevation
451   was not provided for the Colombian dataset so plots were selected based on the forest type, and
452   these plots were excluded from analyses requiring elevation. To avoid double counting plots,
453   Venezuelan and Colombian plots were removed from the ref.[2] dataset.

454

455   **Aboveground carbon**
456   For each tree in the montane dataset we used the published allometric equation by ref.[54] to
457   estimate aboveground biomass. This allometric equation was created using data from directly
458   harvested trees at 58 sites across the tropics, including eight sites with elevation ≥800m asl (range
459   900-3,000m asl including sites in Africa). We then converted this biomass to carbon, assuming that

460 aboveground carbon (AGC, in Mg C ha^{-1}) is 45.6% of aboveground biomass[55]. AGC for each plot was
461 estimated as the sum of the AGC of each living stem, divided by planimetric plot area (in hectares). If
462 field measurements of slope were unavailable, we converted surface to planimetric area extracting
463 slope from the NASA's Shuttle Radar Topography Mission (SRTM) product. We excluded tree ferns,
464 bamboo and palms, as these were not measured in all plots. Ref.[54] includes tree diameter, wood
465 mass density and tree height. The best taxonomic match wood density of each stem was extracted
466 from a global database[56,57] following ref.[53]. For some sites, all trees in a plot had been sampled for
467 height. If this was not the case, but some field measurements of height were available (typically ten
468 stems per diameter class), we constructed a site-specific height-diameter model, using a Weibull
469 equation following ref.[58]. If no field measurements of height were available, we constructed a
470 cluster-specific height-diameter model, using a Weibull equation, as explained in Table S7 in
471 Supplementary Information. The same approach was used to calculate aboveground biomass for
472 lowland forests. For these, height was estimated using a Weibull equation following ref.[58].

473
474 **Small plots and data subsampling**
475 For 22 sites where plots were small (<0.2 ha), we aggregated plots to groups of about 0.2 ha based
476 on their geographic proximity, elevation, environmental affinity and the co-authors' knowledge of
477 the site, to help reduce the variation among plots at site level. This is because the presence of an
478 extremely large tree in a small plot can result in overestimates of AGC[59]. We investigated if using the
479 aggregated-plot approach affected AGC-stock estimates at the site level, and this was not the case
480 (Extended Data Fig. 2). We also investigated if including small plots affected the continental mean
481 AGC-stock estimates, as small plots have greater edge surface, and there is a tendency of some field
482 teams to include large trees inside plots when laying out the boundaries[60]. Including small plots did
483 not significantly affect our continental mean AGC-stock estimates (Extended Data Fig. 2). We also
484 explored the sensitivity of our continental mean AGC-stock estimates to data subsampling. Data
485 were resampled at different sample sizes either at plot level (sampling with replacement) or at site
486 level (sampling without replacement). The number of plots (n=226) and the number of sites (n=44)
487 we sampled indicate that our estimates of AGC-stock at the continental level are robust (Extended
488 Data Fig. 1). They are also not affected by the fact that we included plots 800-1,000 m asl (Extended
489 Data Fig. 3).

490
491 **Size classes**
492 For all plots, we computed the proportion of AGC which was distributed in each size-diameter class,
493 using the classes of ref.[15]. We also computed stem density, basal area, density of large trees (>70 cm
494 diameter, named SD$_{70}$ in stems ha^{-1}) and Podocarpaceae abundance (in percentage of plot-level
495 basal area).

496
497 **Environmental variables and their effects**
498 Climate variables (temperature annual mean and seasonality, and precipitation mean and
499 seasonality, i.e. Bio1, 4, 12 and 15) were extracted from WorldClimV2[61] at 30 arc-sec (~1-km)
500 resolution. Mean temperature values were adjusted for the difference in elevation between the plot
501 and the wider 1-km grid cell using the lapse rate of -0.005°C m^{-1}. We obtained data on cloud cover
502 from ref.[62] and lightning frequency (0.1 degree, ~11 km) from the Lightning Imaging Sensor (LIS) very
503 high resolution climatology[63]. Values for soil variables (cation exchange capacity, CEC, representing
504 soil fertility, and percentage clay representing soil texture) were extracted from SoilGrids[64] (~1-km
505 resolution) and a depth-weighted mean taken for values from 0 to 30 cm depth to give a single value
506 of each soil variable per plot. Elevation was obtained from SRTM (at 3 arc-second resolution, ~90 m).
507 Topographic metrics were calculated from elevation data using the terrain function in the raster R
508 package version 3.3-6. These were slope and topographic position index (TPI). TPI is the difference
509 between the elevation of the plot and the mean value of the eight surrounding grid cells – positive
510 values indicate locally high locations and negative values indicate locally low locations. Where small

511 plots were aggregated for analysis, environmental variables were extracted for the ungrouped plot
512 locations, and then an area-weighted mean taken to obtain a plot-level value.
513
514 **Elephant and conifer effects on AGC-stocks**
515 For the current elephant presence in the AfriMont plots, we created a binary variable
516 (presence/absence) based on co-authors knowledge of elephant ranges and elevation distribution at
517 each site as of 2019. Co-authors estimated that elephants were present in 2019 in 54 plots in 12
518 sites in five countries (see Table S5). For all plots which had at least one individual in the
519 Podocarpaceae family (47 plots, 16 sites, 7 countries), we computed the contribution of
520 Podocarpaceae to plot basal area and AGC-stock in terms of percentages.
521
522 **Estimating forest cover and loss**
523 We obtained estimates of forest cover and loss in the years 2000 through to 2018, using the 'loss
524 year' dataset of the Global Forest Change database, version 1.6 (ref.[38]). To exclude plantation
525 forests, 'dry' forests (e.g. miombo woodland) and degraded forests, we applied the 'primary humid
526 forest' mask developed by ref.[39]. We distinguished montane from lowland forests using an
527 elevational cut-off of 800-m elevation, using the SRTM v3 product at 1 arc-sec resolution (snapping
528 to the ref.[38] grid of the same resolution). Where there were gaps in the 1 arc-sec SRTM product, we
529 filled these using a 1 arc-sec bilinear interpolation of the (gapless) 3 arc-sec SRTM product. Areal
530 estimates of forest cover and loss were calculated at 30-m resolution using the Africa Sinusoidal
531 projection. To estimate future forest loss by year 2030, we extrapolated absolute country-level
532 deforestation rates for the period 2000-2018 (in ha per year).
533
534 **Investigating AfriMont representativeness**
535 To quantify AfriMont sampling effort within the montane forest biome in Africa, we used the map of
536 tropical montane forest extent (see above) and calculated the amount of remaining forest in each 1-
537 degree grid-cell. By dividing the area sampled in the AfriMont dataset by the proportion of this
538 biome in a grid-cell, we calculated the expected sampling intensity if sampling was proportional to
539 remaining forest extent. To assess how representative our plot network was of the environmental
540 conditions of the wider tropical montane forest biome in Africa, we extracted the environmental
541 data (climate and soil variables presented above) at ~1-km resolution from grid-cells that contained
542 montane forest. We then visually compared the distribution of each variable in our dataset to its
543 distribution across the biome (Extended Data Fig. 7).
544
545 **AfriMont vs global AGC maps**
546 We extracted alternative AGC estimates for the AfriMont plots (unaggregated, n=666) from four
547 different sources: Harris et al. (ref.[65]) (30-m resolution, dated 2000), the European Space Agency
548 Climate Change Initiative Biomass map[66] (100-m resolution, 2017), Saatchi, et al. (ref.[67]) (1-km
549 resolution, 2007/8) and Avitabile et al. (ref.[68]) (1-km resolution, circa 2000-2010). Most of the
550 AfriMont plots were sampled between 2000 and 2019 (Table S5). Where the plots were found within
551 a single map pixel, we extracted that value. Where plots were larger than the pixel size, we averaged
552 the values from the surrounding pixels weighted according to the proportion of the pixel that was in
553 the plot.
554
555 **Statistical analysis**
556 Data were analysed using linear mixed-effects models, with site as a random effect. Site was
557 included as a random intercept in all models, and as a random slope where relationships were
558 assessed against elevation. Allowing the slope of the elevation effect to vary amongst sites in this
559 way captures the *a priori* expectation for slopes to differ among sites, for example due to mass
560 elevation effects. The effect of plot size on variation was accounted for by weighting observations by
561 a power transformation of plot size; this was estimated during model fitting using the varPower

562 function in the nlme R package (ref.[69]), and then models refitted using the lme4 R package (ref.[70])
563 using these estimated weights. Confidence intervals and *P*-values for mixed effects models
564 parameters were estimated by bootstrapping models (1,000 iterations) using the
565 bootstrap_parameters function in the parameters R package (ref.[71]). AGC-stocks, stem density and
566 SD_{70} were natural-log transformed (a small constant was added to SD_{70} before log transforming to
567 avoid log-transforming zeros) to meet assumptions of normality and avoid heteroscedacity. Likewise,
568 the proportional contribution of each size class was square-root transformed. Differences in AGC-
569 stocks between all combinations of lowland and montane forests amongst continents were assessed
570 using Tukey post-hoc tests implemented in the multcomp R package (ref.[72]). Relationships between
571 AGC-stocks and environmental variables were investigated by fitting all subsets of the full model
572 with all environmental covariates and averaging the best supported (difference in Akaike
573 information criterion from the best supported model ΔAIC<4) models (using dredge and movel.avg
574 functions in the MuMIn R package (ref.[73]). We used these relationships with climate and soil to
575 predict AGC-stocks in each 1-km grid cell containing montane forests (holding topographic variables
576 at their dataset wide mean), and then took the forest-area weighted mean of these to obtain a
577 single mean for the tropical montane forest biome in Africa. Differences in AGC-stocks between
578 plots with and without elephants were tested using t-test with AGC-stocks natural-log transformed.
579 We investigated if Podocarpaceae abundance (in terms of basal area) and plot AGC-stocks were
580 significantly correlated using Spearman's rank correlation coefficient. To investigate if sampling
581 design affected AfriMont AGC-stock estimates we used ANOVA to test whether site-level mean AGC-
582 stocks differed according to the sampling strategy used to establish plots at that site. To explore the
583 relationship between AfriMont AGC-stock estimates and global maps, and among these global maps,
584 we used Spearman's rank correlation test.

References Methods

50. Lopez-Gonzalez, G., Lewis, S. L., Burkitt, M. & Phillips, O. L. ForestPlots.net: a web application and research tool to manage and analyse tropical forest plot data. *J. Veg. Sci.* **22**, 610–613 (2011).

51. Lopez-Gonzalez, G., Lewis, S. L., Burkitt, M., Baker, T. R. & Phillips, O. L. ForestPlots.net Database http://www.forestplots.net (2009).

52. Cavanaugh, K., et al. Carbon storage in tropical forests correlates with taxonomic diversity and functional dominance on a global scale. *Global Ecol. Biogeogr.* **23**, 563-573 (2014).

53. Lewis, S. L., et al. 2009 Increasing carbon storage in intact African tropical forests. *Nature* **457**, 1003–1006 (2009).

54. Chave, J. et al. Improved allometric models to estimate the aboveground biomass of tropical trees. *Glob. Change Biol.* **20**, 3177–3190 (2014).

55. Martin, A. R., Doraisami, M. & Thomas, S. C. Global patterns in wood carbon concentration across the world's trees and forests. *Nat. Geosci.* **11**, 915–920 (2018).

56. Chave, J. et al. Towards a worldwide wood economics spectrum. *Ecol. Lett.* **12**, 351–366 (2009).

57. Zanne, A. E. et al. Towards a Worldwide Wood Economics Spectrum https://doi.org/10.5061/dryad.234 (Dryad Digital Repository, 2009).

58. Clark, D.A., Brown, S., Kicklighter, D.W., Chambers, J.Q., Thomlinson, J.R., Ni, J. & Holland, E.A. Net primary production in tropical forests: an evaluation and synthesis of existing field data. *Ecol. Appl.* **11**, 371–384 (2001).

59. Paul, T.S.H., Kimberley, M.O. & Beets, P.N. Thinking outside the square: Evidence that plot shape and layout in forest inventories can bias estimates of stand metrics. *Methods Ecol. Evol.* **10**, 381–388 (2019).

60. Fick, S.E. & Hijmans, R.J., WorldClim 2: new 1-km spatial resolution climate surfaces for global land areas. *Int. J. Climatol.* **37**, 4302–4315 (2017).

612 61. Wilson, A.M. & Jetz, W. Remotely sensed high-resolution Global Cloud Dynamics for
613   predicting ecosystem and biodiversity distributions. *PLoS Biol* **14**(3): e1002415 (2016).
614 62. Albrecht, R., Goodman, S., Buechler, D., Blakeslee R. & Christian, H. LIS 0.1 Degree Very High
615   Resolution Gridded Lightning Climatology Data Collection. Data sets available online
616   [https://ghrc.nsstc.nasa.gov/pub/lis/climatology/LIS/] from the NASA Global Hydrology
617   Resource Center DAAC, Huntsville, Alabama, U.S.A. doi:
618   http://dx.doi.org/10.5067/LIS/LIS/DATA306
619 63. Hengl, T., et al. SoilGrids250m: Global gridded soil information based on machine learning.
620   *PLoS ONE* **12**(2): e0169748 (2017).
621 64. Harris, N. L. et al. Global maps of twenty-first century forest carbon fluxes. *Nat. Clim. Change*
622   **11**, 234–240 (2021).
623 65. Santoro, M. & Cartus, O. ESA Biomass Climate Change Initiative (Biomass_cci): Global
624   datasets of forest above-ground biomass for the year 2017, v1. Centre for Environmental
625   Data Analysis, 2019. doi:10.5285/bedc59f37c9545c981a839eb552e4084
626 66. Saatchi, S., et al. Benchmark map of forest carbon stocks in tropical regions across three
627   continents. *PNAS* **108**, 9899-9904 (2011).
628 67. Avitabile, V., et al. An integrated pan-tropical biomass map using multiple reference
629   datasets. *Glob. Change Biol.* **22**, 1406–1420 (2016).
630 68. Pinheiro, J., Bates, D., DebRoy, S., Sarkar, D. & R Core Team. nlme: Linear and Nonlinear
631   Mixed Effects Models. R package version 3.1-151, https://CRAN (2020).
632 69. Bates, D. Maechler, M., Bolker B. & Walker, S. Fitting Linear Mixed-Effects Models Using
633   lme4. *J. Stat. Softw.* **67**, 1–48 (2015).
634 70. Lüdecke, D., Ben-Shachar, M., Patil, I. & Makowski, D. Parameters: extracting, computing
635   and exploring the parameters of statistical models using R. *J. Open Source Softw* **5**, 2445
636   (2020).
637 71. Hothorn, T., Bretz, F. & Westfall, P. Simultaneous Inference in General Parametric Models.
638   *Biometrical Journal* **50**, 346–363 (2008).
639 72. Barton, K. 2020. MuMIn: Multi-Model Inference. R package version 1.43.17.
640

Acknowledgements

710 **Author Contributions**
711 A.C-S. conceived the study and assembled the AfriMont dataset. A.C-S. and M.J.P.S. analysed the
712 plot data (with contributions from S.L.L.) and wrote the manuscript. P.J.P. analysed forest extents
713 and contributed to writing. S.L.L. conceived and managed the AfriTRON forest plot recensus

714 programme. E.T.A.M. and V.A. helped compare plot data with remote sensing carbon maps. All co-
715 authors read and approved the manuscript.
716
718
719 **Additional information**
720 Supplementary information is available for this paper at XX (to be added)
721 Correspondence and requests for materials should be addressed to A. C-S.
722 Reprints and permissions information are available at XX (to be added)
723
724 **Data availability**
725 Source data to generate figures and tables are available from:
726 https://doi.org/10.5521/forestplots.net/2021_5
727
728 **Code availability**
729 R code to generate figures and tables is available from:
730 https://doi.org/10.5521/forestplots.net/2021_5
731

732 **Affiliations**
733 [1]Department of Environment and Geography, University of York, York, UK. [2]Department of
734 International Environmental and Development Studies (NORAGRIC), Norwegian University of Life
735 Sciences, Ås, Norway. [3]Department of Natural Sciences, Manchester Metropolitan University,
736 Manchester, UK. [4]School of Geography, University of Leeds, Leeds, UK. [5]Climate Change Specialist
737 Group, Species Survival Commission, International Union for Conservation of Nature, Gland,
738 Switzerland. [6]University College London, Department of Geography, London, UK. [7]Biology
739 Department, Université Officielle de Bukavu, Bukavu, DRC. [8]Service of Wood Biology, Royal Museum
740 for Central Africa, Tervuren, Belgium. [9]Department of Environment, Laboratory of Wood Technology
741 (Woodlab), Ghent University, Ghent, Belgium. [10]University of Jos, Jos, Nigeria. [11]Nigerian Montane
742 Forest Project, Taraba State, Nigeria. [12]Department of Geosciences and Geography, University of
743 Helsinki, Finland. [13]Department of Zoology, Faculty of Science, Charles University, Prague, Czech
744 Republic. [14]Institute of Vertebrate Biology, Czech Academy of Sciences, Brno, Czech Republic.
745 [15]Institute of Botany of the Czech Academy of Science, Třeboň, Czech Republic. [16]College of Natural
746 and Computational Science, Addis Ababa University, Addis Ababa, Ethiopia. [17]Department of Natural
747 Resource Management, College of Agriculture and Natural Resource, Wolkite University, Wolkite,
748 Ethiopia. [18]European Commission, Joint Research Centre, Ispra, Italy. [19]UK Centre for Ecology &
749 Hydrology, Edinburgh, UK. [20]Université du Cinquantenaire Lwiro, Département de sciences de
750 l'environnement, Kabare, Suk-Kivu, DRC. [21]Isotope Bioscience Laboratory (ISOFYS), Ghent University,
751 Ghent, Belgium. [22]Plant Systematic and Ecology Laboratory, Higher Teachers' Training College,
752 University of Yaoundé I, Yaoundé, Cameroon. [23]Institute of Tropical Forest Conservation, Mbarara
753 University of Science and Technology, Uganda. [24]Biodiversity and Landscape Unit, Gembloux Agro-
754 Bio Tech, Université de Liege, Liège, Belgium. [25]Institut for Geography, Friedrich-Alexander-
755 Universität, Erlangen-Nürnberg, Germany. [26]Institut Supérieur d'Agroforesterie et de Gestion de
756 l'Environnement de Kahuzi-Biega (ISAGE-KB); Département de Eaux et Forêts, Kalehe, DRC. [27]UN
757 Environment World Conservation Monitoring Center (UNEP-WCMC), Cambridge, UK.
758 [28]Computational & Applied Vegetation Ecology (CAVElab), Faculty of Bioscience Engineering, Ghent
759 University, Ghent, Belgium. [29]Department of Anthropology, George Washington University,
760 Washington DC, USA. [30]School of Life Sciences, University of KwaZulu-Natal, Scottsville,
761 Pietermaritzburg, South Africa. [31]Shaanxi Key Laboratory for Animal Conservation, Northwest
762 University, Xi'an, China. [32]International Centre of Biodiversity and Primate Conservation, Dali
763 University, Dali Yunnan, China. [33]University of Canterbury, New Zealand. [34]Inventory & Monitoring
764 Program, National Park Service, Fredericksburg, USA. [35]University of Ghent, Belgium. [36]World

765 Agroforestry (ICRAF), Nairobi, Kenya. [37]Laboratory of Geo-Information Science and Remote Sensing,
766 Wageningen University, Wageningen, the Netherlands. [38]Geography, Environment & Geomatics,
767 University of Guelph, Canada.[39]Faculty of Science, University of South Bohemia, České Budějovice,
768 Czech Republic. [40]AMAP Lab, Université de Montpellier, IRD, CNRS, INRAE, CIRAD, Montpellier,
769 France.[41]Faculté de Gestion de Ressources Naturelles Renouvelables, Université de Kisangani,
770 Kisangani, DRC. [42]College of Development Studies, Addis Ababa University, Ethiopia.
771 [43]Dendrochronology Laboratory, World Agroforestry Centre (ICRAF), Kenya. [44]Missouri Botanical
772 Garden, St. Louis, Missouri, USA. [45]Department of Biology, University of Burundi, Burundi.
773 [46]Smithsonian Institution Forest Global Earth Observatory (ForestGEO), Smithsonian Tropical
774 Research Institute, Washington DC, USA. [47]Kunming Institute of Botany, Kunming, China. [48]Université
775 Libre de Bruxelles, Brussels, Belgium. [49]Division of Vertebrate Zoology, Yale Peabody Museum of
776 Natural History, New Haven, CT, USA. [50]Institute for Atmospheric and Earth System Research, Faculty
777 of Science, University of Helsinki, Finland. [51]Department of Plant Systematics, University of Bayreuth,
778 Germany. [52]Institute for Geography, Friedrich-Alexander-University Erlangen-Nuremberg, Germany.
779 [53]Helmholtz-Centre for Environmental Research (UFZ), Leipzig, Germany. [54]Department of Ecology,
780 Faculty of Science, Charles University, Prague, Czech Republic. [55]International Gorilla Conservation
781 Programme, Musanze, Rwanda. [56]Department of Natural Resources, Karatina University, Kenya.
782 [57]Dept. Ecosystem Science & Sustainability, Colorado State University, Fort Collins, USA.
783 [58]Eco2librium LLC, Boise, USA. [59]Department of Ecology, Université de Kisangani, Kisangani, DRC.
784 [60]Environmental Change Institute, School of Geography and the Environment, University of Oxford,
785 Oxford, UK. [61]Tropical Forests and People Research Centre, University of the Sunshine Coast,
786 Australia. [62]Flamingo Land Ltd., North Yorkshire, UK. [63]College of African Wildlife Management,
787 Mweka, Tanzania. [64]School of GeoSciences, University of Edinburgh, UK. [65]Department of Geography
788 and Environmental Sciences, University of Dundee, Dundee, UK. [66]Independent Botanist, Harare,
789 Zimbabwe. [67]Department of Horticultural Sciences, Faculty of Applied Sciences, Cape Peninsula
790 University of Technology, Bellville, South Africa. [68]Biology Department, University of Rwanda,
791 Rwanda. [69]Department of Biological and Environmental Sciences, University of Gothenburg, Sweden.
792 [70]Mountains of the Moon University, Fort Portal, Uganda. [71]National Agricultural Research
793 Organisation, Mbarara Zonal Agricultural Research and Development Institute, Mbarara, Uganda.
794 [72]School of Biological Sciences, University of Southampton, Southampton, UK. [73]Conservation
795 Science Group, Department of Zoology, University of Cambridge, Cambridge, UK. [74]State Key
796 Laboratory of Information Engineering in Surveying, Mapping and Remote Sensing, Wuhan
797 University, China. [75]Key Biodiversity Areas Secretariat, BirdLife International, Cambridge, UK.
798 [76]School of Life Sciences, University of Lincoln, UK. [77]Department of Biology, University of Florence,
799 Sesto Fiorentino, Italy. [78]Tropical Biodiversity Section, Museo delle Scienze, Trento, Italy. [79]Tropical
800 Plant Exploration Group (TroPEG) Cameroon. [80]Center for Development Research (ZEF), University of
801 Bonn, Germany. [81]Conservation and Landscape Ecology, University of Freiburg, Germany.[82]Applied
802 Biology and Ecology Research Unit, University of Dschang, Dschang, Cameroon. [83]Forest Ecology and
803 Forest Management Group, Wageningen University, Wageningen, The Netherlands. [84]Water and
804 Land Resources Center, Addis Ababa University, Addis Ababa, Ethiopia. [85]African Wildlife Foundation
805 (AWF), Biodiversity Conservation and Landscape Management Program, Simien Mountains National
806 Park, Debark, Ethiopia. [86]Faculty of Forestry, University of British Columbia, Vancouver, Canada.
807 [87]Center for International Forestry Research (CIFOR), Bogor, Indonesia. [88]Department of Forest
808 Ecology, Faculty of Forestry and Wood Sciences, Czech University of Life Sciences, Prague, Czech
809 Republic. [89]Department of Plant Biology, Faculty of Sciences, University of Yaoundé I, Cameroon.
810 [90]Bioversity International, Yaoundé, Cameroon. [91]UK Research & Innovation, UK. [92]Department of
811 Geography, National University of Singapore, Singapore. [93]Institute of Forestry and Conservation,
812 University of Toronto, Toronto, Canada.[94]Biodiversity Foundation for Africa, East Dean, East Sussex,
813 UK. [95]Forestry Development Authority of the Government of Liberia (FDA), Monrovia, Liberia.
814 [96]School of Forestry and Environmental Studies, Yale University, New Haven, USA. [97]Department of
815 Biological Sciences, Florida International University, Florida, USA. [98]School of Natural Sciences,

816   University of Bangor, Bangor, UK. [99]Rothamsted Research, Harpenden, UK. [100]University of Liberia,
817   Monrovia, Liberia. *corresponding author: a.cuni-sanchez@york.ac.uk
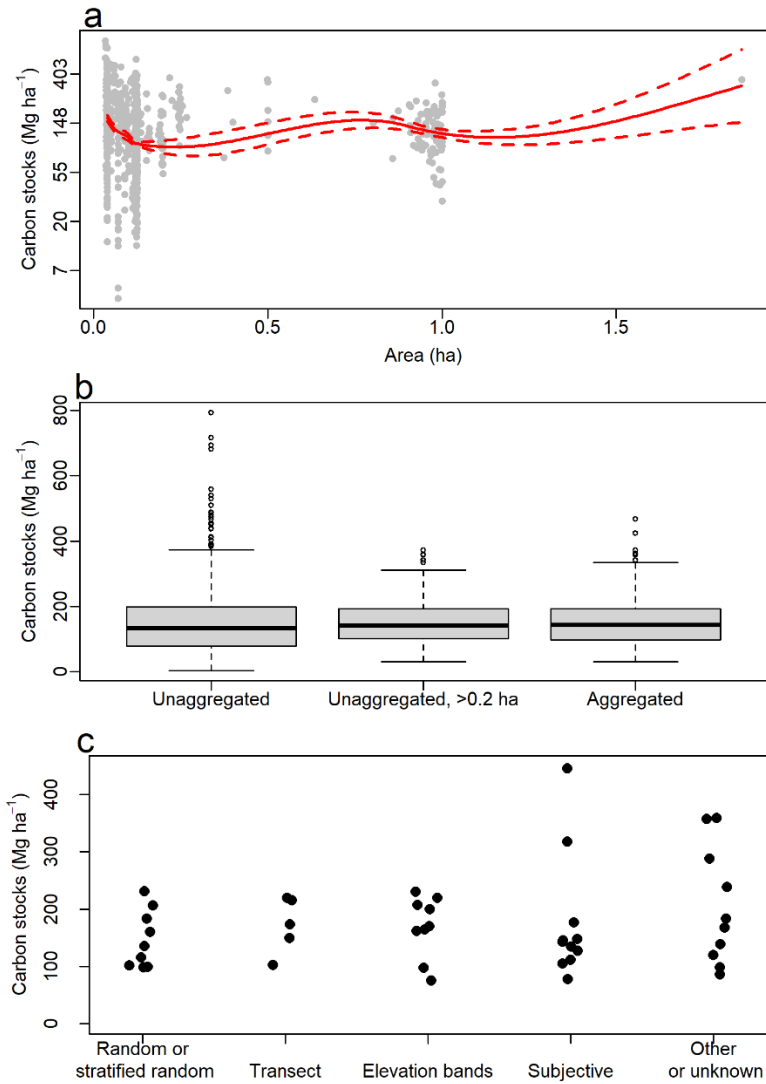
818

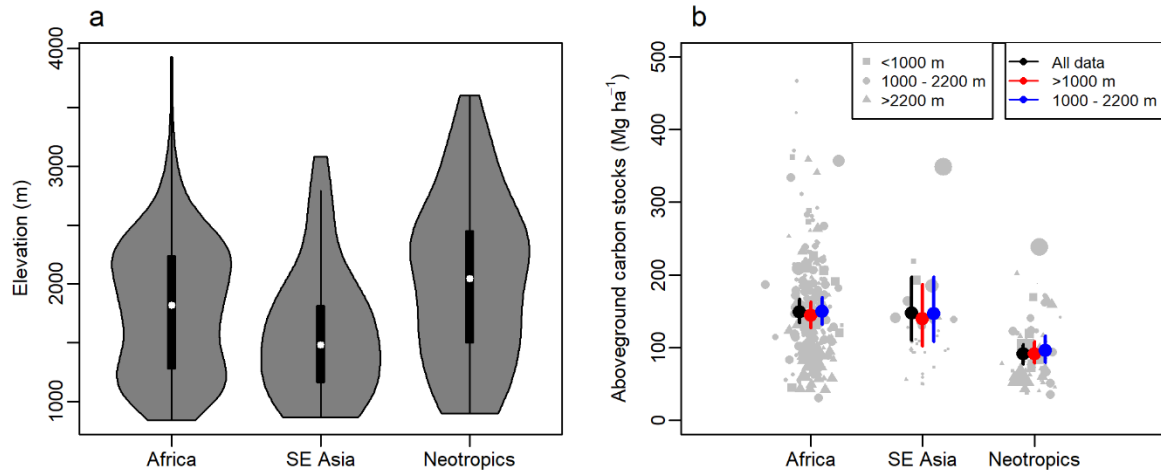819   **Extended Data**

820
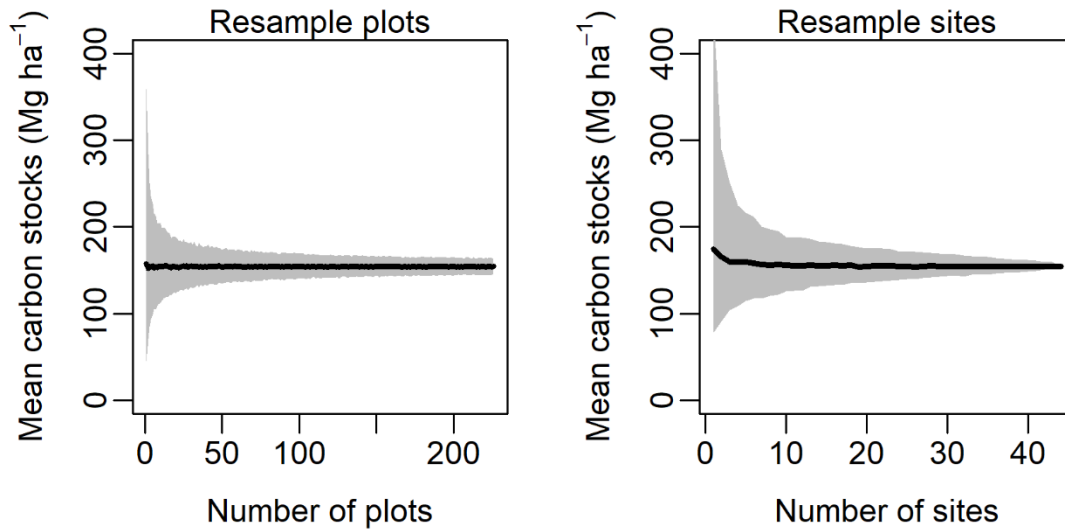
821

822   **Extended Data Fig. 1 | Sensitivity of mean aboveground carbon stock estimates to data**
823   **subsampling.** AfriMont plot data were resampled at different sample sizes either at plot level
824   (sampling with replacement) or at site level (sampling without replacement). *N* = 1,000 resamples
825   for each sample size.

826

827

Extended Data Fig. 2 | Effect of plot area, aggregation procedure and plot design on estimates of aboveground carbon stocks across the AfriMont plot network. (**a**) Relationship between aboveground carbon stocks and plot area of plots prior to aggregation. The red line shows the fit of a locally weighted regression model (span = 0.75) relating these variables, with dashed lines showing the standard errors. (**b**) Variation in aboveground carbon stocks using either all plots prior to aggregation (unaggregated), plots prior to aggregation but excluding those < 0.2 ha (unaggregated, > 0.2 ha) or the aggregated plots used in the main analyses (aggregated). (**c**) Effects of plot design on aboveground carbon stocks (each site represents one dot). Sampling strategies include random or stratified random, plots positioned along transects, plots established within elevation bands, subjective measures such as choosing an area of forest considered representative of the wider area, and other strategies (one plot sampled per site or unclear strategy). Carbon stocks (log-transformed) did not differ significantly between sites with different sampling strategies (ANOVA: $F_{4,39}$ = 0.432, P = 0.785). For specific site information see Table S5.

841

842

843

Extended Data Fig. 3 | Robustness of differences in tropical montane forest aboveground carbon (AGC) stocks among continents based on plot networks to differences in elevation. (**a**) Elevations of montane forests plots sampled in each continent. Violin plots show the distribution of data, with boxplots showing the median and interquartile range of elevation in each continent. (**b**) Effect of removing submontane plots (800-1,000 m asl) and high elevation plots (> 2,200 m asl, approximately the upper quartile of elevations for the African montane plot dataset) on AGC-stocks in montane forests sampled by plot networks in each continent. Mean AGC-stocks and 95% confidence intervals are shown as estimated by models using i) all data, ii) excluding plots 800-1,000 m, and iii) restricting plots to 1,000-2,200 m. Means for all plots differ from the analysis in Fig. 1 as literature plots without elevation data (plots in Colombia) were excluded from this analysis. Point symbols are proportional to square-root plot area. *N* = 324 plots.

855

856
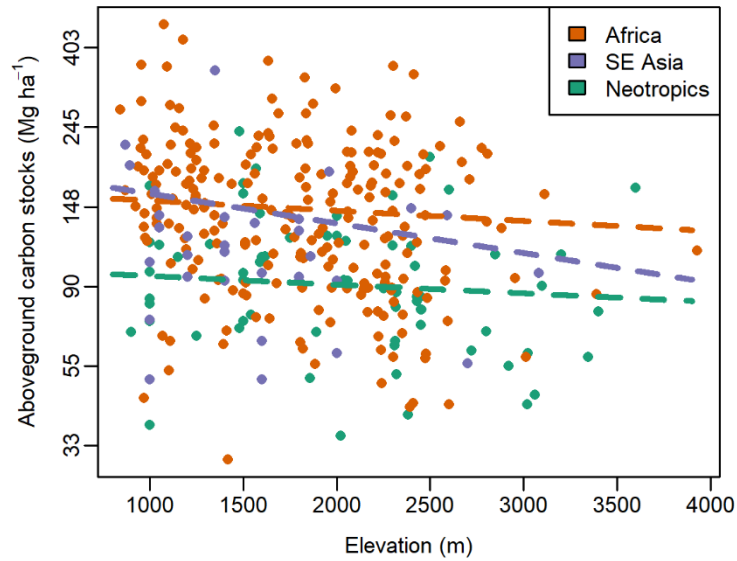
857
858 **Extended Data Fig. 4 | Relationship between aboveground carbon (AGC) stocks and elevation for**
859 **tropical montane forests in each continent based on plot networks.** Dashed lines show
860 relationships from a linear mixed-effects model of log-transformed AGC-stocks as a function of
861 elevation, continent and their interaction. Site was included as a random effect, and AGC-stock –
862 elevation relationships allowed to vary among sites. Lines show fitted slopes across sites. Neither the
863 overall relationship between elevation and AGC-stocks (slope = -0.039 [95% CI = -0.127 – 0.057], P =
864 0.420) nor interactions between elevation and continent (Southeast Asia, change in slope = -0.074 [-
865 0.294 – 0.149], P = 0.503; Neotropics, change in slope = 0.006 [-0.132 – 0.149], P = 0.913) are
866 statistically significant. N = 324 plots.
867
868
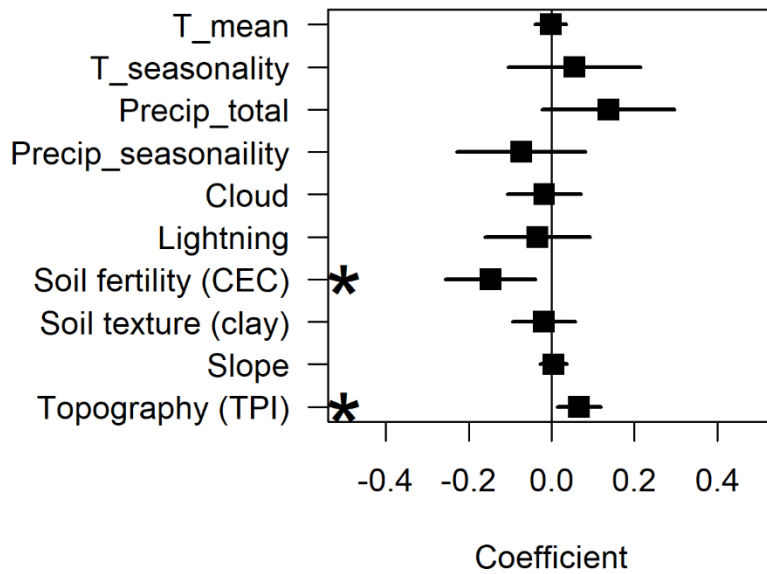
Extended Data Fig. 5 | Environmental drivers of aboveground carbon stocks across the AfriMont plot network. Coefficients are from a linear mixed-effects model with site as a random intercept. Results are following all-subsets regression and model averaging, in which variables that do not appear in well supported models are given coefficients of zero, leading to shrinkage in model coefficients. Statistically significant relationships ($P < 0.05$) are indicated with asterisks. TPI refers to topographic position index (positive values indicate higher than surroundings, negative values indicate lower than surroundings). T_mean: annual mean temperature, T_seasonality: temperature seasonality, Precip_total: annual precipitation, Precip_seasonality: precipitation seasonality.
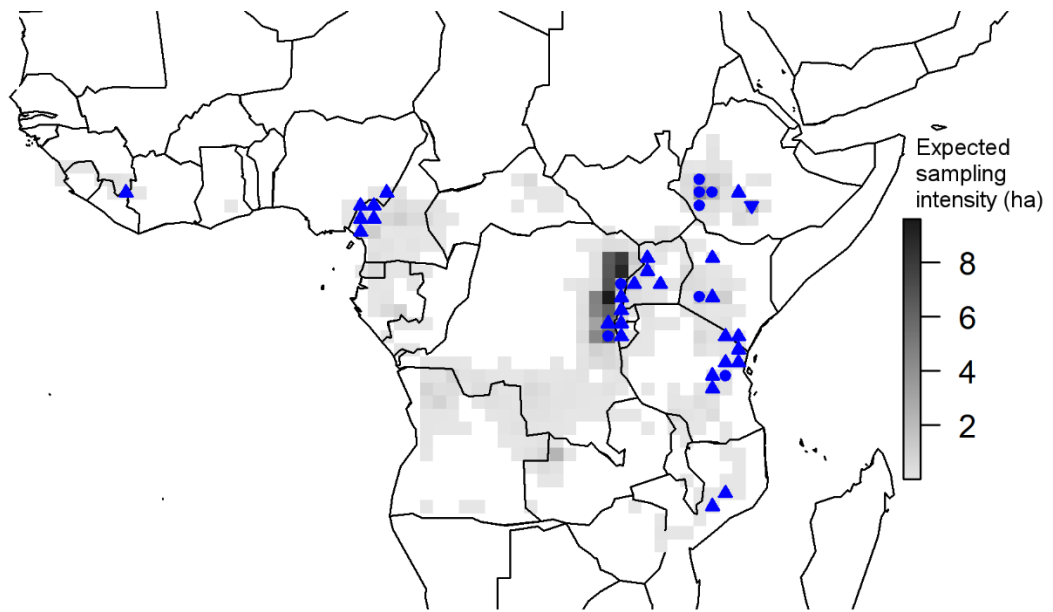
880
881 **Extended Data Fig. 6 | Expected sampling effort if effort was distributed in proportion to the area**
882 **of tropical montane forest biome in Africa.** Data are summarised at 1-degree resolution. Upward
883 triangles show grid-cells where AfriMont sampling effort is more than double expected effort,
884 downward triangles show grid-cells where AfriMont sampling effort is less than half expected effort.
885 Circles denote AfriMont sampling effort being between half and double expected effort. The extent
886 of the tropical montane forest biome was defined as closed-canopy forests ≥ 800 m asl in December
887 2018, extracted from ref.[38] and clipped to 'primary humid forest' using ref.[39]. This grided map differs
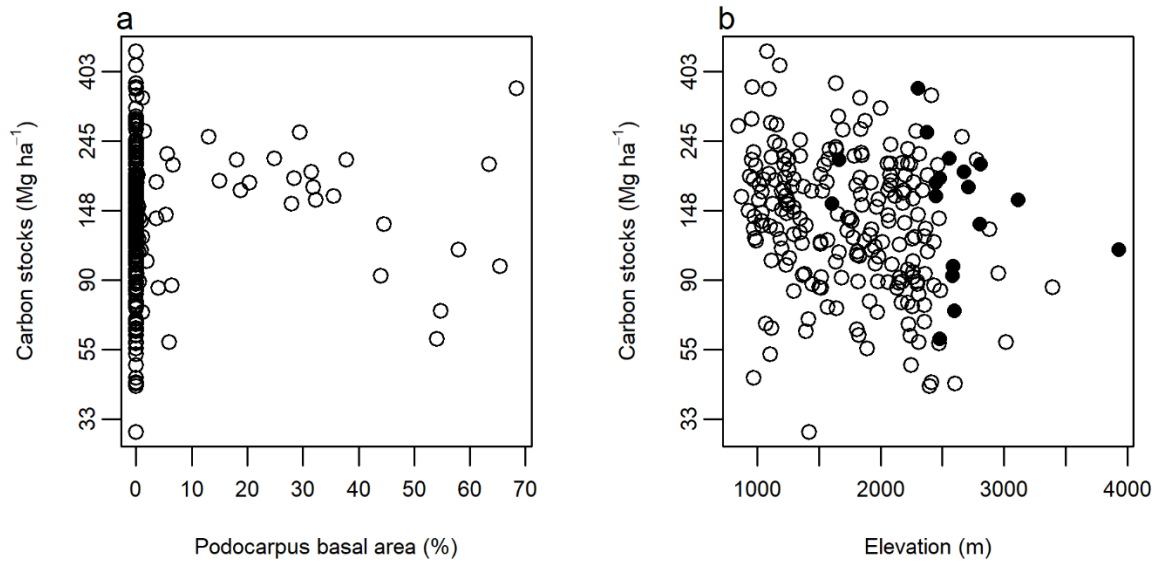888 from Fig. 4 as numerous grids have very little tropical montane forest.
889
890
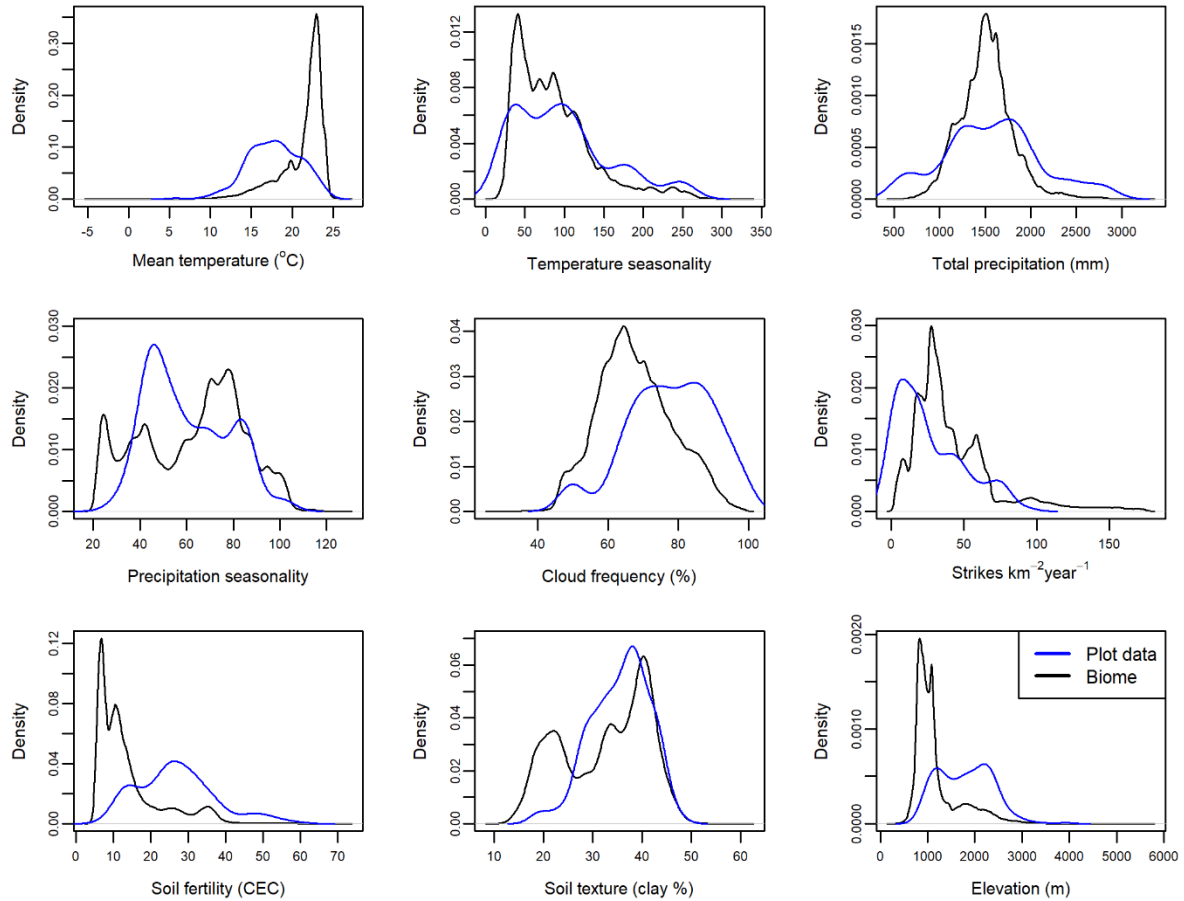
891
**Extended Data Fig. 7 | Differences in the environmental conditions sampled by the AfriMont plot
network and the tropical montane forest biome in Africa.** The extent of the biome was defined as
closed-canopy forests ≥ 800m asl in December 2018, extracted from ref.[38] and clipped to 'primary
humid forest' using ref.[39]. Environmental variables for the biome were extracted at ~1-km
resolution.
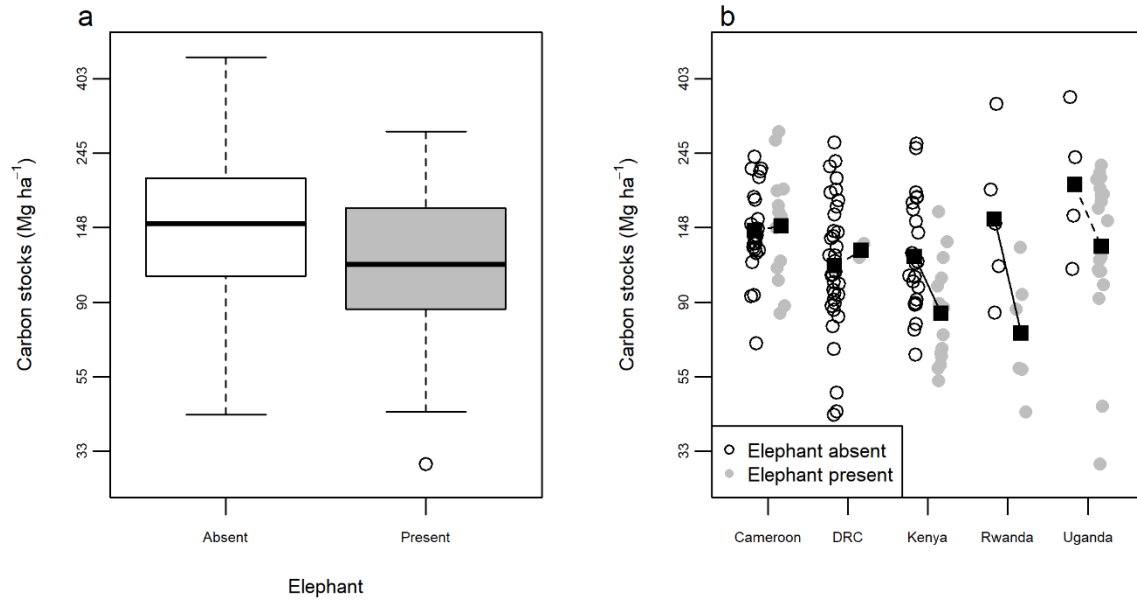
899
900 **Extended Data Fig. 8 | Differences in aboveground carbon (AGC) stocks in AfriMont plots located in**
901 **montane forests with and without elephants. a)** Differences across all plots. AGC-stocks are
902 statistically significantly lower in forests with elephants (*t*-test, t = 3.5, df=83.5, *P* = 0.001). The thick
903 line shows the median, and boxes cover the interquartile range (IQR). Values > 1.5 times IQR away
904 from the IQR are shown by points. **b)** Differences in countries where elephants are present in at least
905 one of the montane sites studied. Black squares show means in each country in forests with or
906 without elephants – solid lines denote statistically significant differences (*t*-tests, *P* < 0.05). Elephant
907 presence in 2019 was estimated by co-authors (see Table S5).
908
909

910
911 **Extended Data Fig. 9 | Relationship between aboveground carbon (AGC) stocks and**
912 **Podocarpaceae.** (**a**) Relationship between AGC-stocks and Podocarpaceae basal area across plots in
913 the AfriMont network, expressed as a percentage of total plot basal area. These variables are not
914 significantly correlated (r_s = 0.083, n = 226, P = 0.212). (**b**) Distribution of plots with at least 20%
915 basal area of Podocarpaceae (black points) in relation to elevation and AGC-stocks. AGC-stocks are
916 not significantly related to elevation or Podocarpaceae basal area (Linear mixed effects model, P =
917 0.152 and 0.132 respectively).
918
919
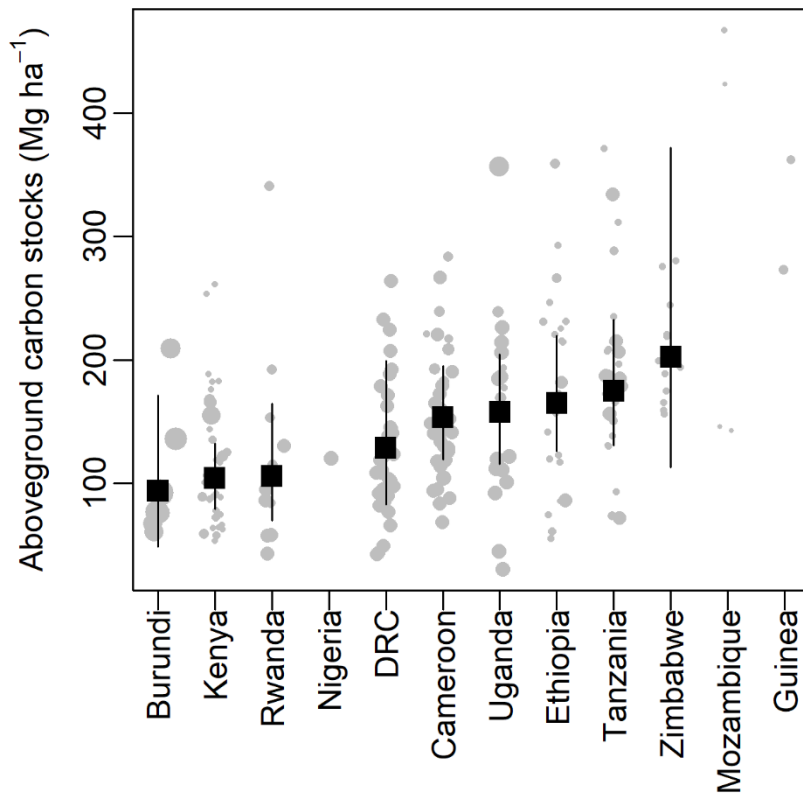
Extended Data Fig. 10 | Within country variation in aboveground carbon stocks based on the AfriMont plot network. Error bars show means and 95% confidence intervals estimated by linear mixed-effects models. Modelled means not shown for countries with fewer than five plots. Point size is proportional to plot area.